Max-Planck-Institut für Plasmaphysik, EURATOM Association, Greifswald

ON NON-LOCAL EFFECTS OF ECE MEASUREMENTS AT W7-AS

N.B. Marushchenko, H. Maaßberg, H. Hartfuß, A. Dinklage

1 Introduction

The basic assumptions of "standard" ECE electron temperature measurements are i) highly localized emission in a sufficiently narrow frequency range (frequency band of the reciever), and ii) the equivalence of the spectral intensity and the local electron temperature.
In high power ECRH discharges at low densities, a population of suprathermal electrons appears in the deposition region, which can significantly affect the ECE spectrum making the interpretation more complex. But even without suprathermal emission, it is necessary to determine the spatial resolution of ECE measurements and the impact on the T_e profile evaluation [1].

The aim of this work is to estimate the limitation of the spatial resolution in the ECE diagnostic coming from the intrinsic non-locality of the EC emission.

This analysis is important for the concept of the ECE evaluation in the new generation stellarator W7-X (under construction in Greifswald, Germany), and we must avoid these problems in the "standard" ECE evaluation where the spectral intensity,I_ω, measured in a narrow frequency channel, ω, is interpreted as the "local" electron temperature. As an example, where the non-local effects of the ECE are fairly strong, a W7-AS discharge with a highly peaked T_e profile is analysed.

The ECE measurements at W7-AS were performed by a radiometer at the 2nd harmonic X-mode which is positioned at the low-field-side lfs. Plasma is optically thick for the X2-mode, and for rather low electron temperatures ($T_e \lesssim 1$ keV), mainly the characteristics of radiometer (are responsible for the spatial resolution δR of the ECE measurements. In the local ("cold") approach, the spatial resolution can be estimated as $\delta R_c \simeq \delta f/f \cdot B(\partial B/\partial R)^{-1}$, which for the bandwidth of $\delta f = 0.3$ GHz should give a perfect spatial resolution, $\delta R_c \simeq 2$ mm.

2 Origin of ECE non-localities

Two effects are responsible for the ECE line broadening measured outside of the plasma:
i) the relativistic effect leading to a frequency down-shift, and
ii) the reabsorption at lower B, i.e. close to the "cold resonance".
Consequently, the measured spectral intensity, I_ω, is determined by the balance of both effects.

This means, that a "local" interpretation of the measured I_ω spectra leads to a systematic inward-shift to higher B (with respect to the "cold resonance" position), and that the spatial resolution is always smaller than the local ("cold") one, i.e. $\delta R_r > \delta R_c$.
Estimation of the spatial resolution for slightly relativistic electrons leads to
$\delta R_r \simeq \delta R_c + T_e/mc^2 \cdot B(\partial B/\partial R)^{-1}$, and $\delta R_r \simeq 1$ cm is obtained for $T_e = 5$ keV compared to $\delta R_c \simeq 2$ mm in the "cold" (standard) approach.
The radiative transport equation [2] can be written in the form

$$I_\omega(s) = I_\omega^{inc}(-a)\,\mathrm{e}^{-\tau_\omega(s)} + \int_{-a}^{s} \mathrm{d}s'\,\eta_\omega(s')\,\mathrm{e}^{-(\tau_\omega(s)-\tau_\omega(s'))} \qquad (1)$$

where I_ω is the spectral intensity, τ_ω is the optical depth [3] defined as the absorption coefficient, α_ω, integrated along the chordup to s, and η_ω is the emission coefficient. For a Maxwellian distribution function there is the relation: $\eta_\omega = \omega^2/8\pi^3c^2 \cdot T_e\,\alpha_\omega$.

Assuming a very high optical depth close to the "cold resonance" layer and a fairly flat $T_e(s') \simeq T_e(s)$, Eq.(1) can be reduced to the usual definition of the radiative temperature, $I_\omega(a) \simeq C\,T_e(s_*)$, where the location of emission, s_*, is usually approximated by the "cold resonance" condition. Exactly the last relation is the usual basis for the ECE diagnostics.
The local absorption coefficient scales roughly with $\alpha_\omega(s') \propto n_e(s')T_e(s')$, thus $\eta_\omega(s') \propto n_e(s')T_e^2(s')$ strongly increases with T_e.

For stronger gradients $\partial T_e/\partial s'$ two effects are observed: i) the value of the radiative temperature, T_{rad}, is an average over the emission region weighted by the exponential in the integrand of Eq.(1) which describes the reabsorption, and ii) the location of emission, s_*, is additionally shifted, where this additional shift has different signs for the hfs and lfs.

For the hfs, the T_e reduces the non-locality ($\partial B/\partial s'$ and $\partial T_e/\partial s'$ have different signs) whereas for the lfs measurements the non-locality is increased. Then the "local" T_{rad} estimation for the hfs is more reliable compared to the lfs. This tendency strengthens also the asymmetric spatial resolutions from the "cold" definition for δR_c due to the higher B-gradient on the hfs.

Consequently, non-local effects can contribute mainly at the lower frequency channels for the ECE interpretation.

3 Simulations

The spectral intensity $I_\omega = I_\omega(a)$ is calculated with given $n_e(r)$ and $T_e(r)$ profiles which are mapped to the horizontal ECE chord (straight line assumed) with $N_\parallel = 0$. I_ω is averaged (integrated) with respect to the finite band width of all ECE frequency channels, obtaining $\overline{I_\omega}$. An averaged T_{rad} profile is obtained from the simulated I_ω spectrum, which can be compared with the measured ECE data; see Fig. 1.

Since the balance of emission and reabsorption is fairy asymmetric with respect to this maximum in s', an integral definition appears to be appropriate: the position s_* is defined by $\overline{I_\omega}(s_*) = 0.5\,\overline{I_\omega}$ for the central frequency ("weighted center" of the emission line). This definition leads to an additional "inward-shift". The spatial extension of the emission zone for each channel is defined as the range with 90% contribution to the (central) I_ω. Then, the bounds s_{min} and s_{max}, are obtained from the conditions $I_\omega(s_{min}) = 0.05\,I_\omega$ and $I_\omega(s_{max}) = 0.95\,I_\omega$.

A low density ($n_e \simeq 2\,10^{19}$ m^{-3}) ECRH discharge (1.2 MW heating with X2-mode at 140 GHz) with high temperature ($T_e \simeq 6$ keV) and very steep gradient (T_e' nearly 1 keV/cm) is a well suited scenario for the analysis. The highly focused ECRH with on-axis deposition results in a highly peaked T_e profile; see Ref. [4]. A suprathermal electron population is clearly indicated in the low frequency channels of the ECE diagnostic; see Fig. 1. The simulated T_{rad} spectrum is calculated with given n_e and T_e profiles (fits to Thomson scattering and ECE data). The simulation is performed for all 24 ECE channels covering the range from 130 to 153 GHz (with a gap around the ECRH frequency at 140 GHz). Omitting the β-effects in the coordinate transform acts like outward-shift (to lower frequencies) of the T_{rad} spectrum. With a sufficiently accurate transform, however, $T_e(r)$ profiles can be mapped to all frequency channels of an ECE system within a fitting procedure. Then, the simulated and the measured $\overline{I_\omega}$ are compared, and the problem of the non-locality of the emission is completely treated. All inaccuracies with the positioning of a "local" T_{rad} value for only one ECE channel diasappears. This approach is used within the integrated data analysis (IDA) concept for W7-X.

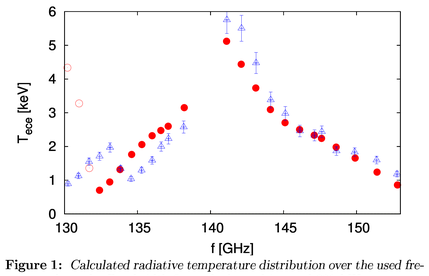

Figure 1: *Calculated radiative temperature distribution over the used frequency channels. Bandwidth for each channel is equal 300 MHz.*

As an illustration, profiles of the absorbtion coefficient $\alpha_\omega(R)$ (reabsorption omitted) are shown in Fig. 2a for three different channels.
For two channels, the "cold" resonance is located nearly symmetrically in r (i.e. to nearly identical n_e and T_e), and the last one corresponds to an outer radius with the non-thermal feature.

The shape of $\alpha_\omega(R)$ for the high-field-side channel is very narrow, but much broader for the corresponding low-field-side one.

The decreased $\partial B/\partial R$ at the low-field-side one cannot explain alone this effect, the strong gradients of T_e are mainly responsible for this difference.

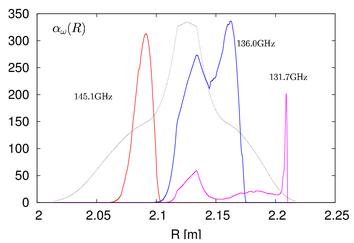

Figure 2a: *Absorbtion coefficient profiles for the different frequency channels. For comparison the inferred $T_e(R)$ profile is also shown.*

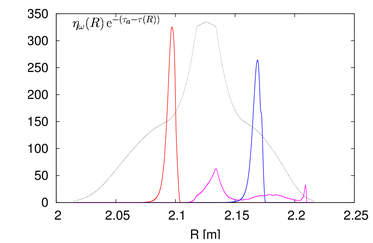

Figure 2b: *Emissivity supressed by reabsorbsed (integrand function from Eq.(1)) for the same as in Fig.2a frequency channels.*

With mapping from frequency channels to the major radius R, $T_{rad}(R)$ is shown in Fig. 3.

As expected, the profile $T_{rad}(R_*)$ with the non-local emission positioning has a significant hfs shift with respect to the profile in local ("cold") approach.

The radial bars given in Fig. 3, determinate for each channel the spatial resolution of ECE diagnostic (defined equivalent to s_{min} and s_{max}). The "cold" resonance definition of R almost coincides with the right-side bar, while the left-side bars determine the real width of the emission line.

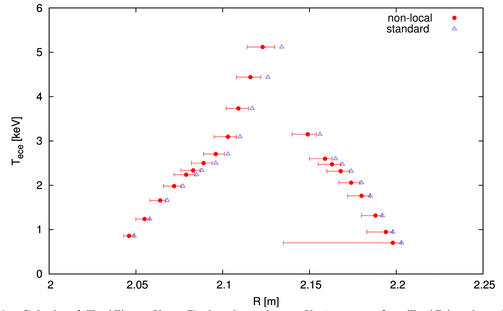

Figure 3: *Calculated $T_{rad}(R)$ profiles. Circles show the profile interpreted as $T_{rad}(R_*)$, where R_* is the emission location; triangles show the same profile, but interpreted as standard one, $T_{rad}(R_c)$ with R_c taken as the "cold" resonance location.*

Please note, that the radial bars on the hfs are smaller than in lfs, especially on periphery.

The size of the spatial resolution is noticably higher than the one obtained from the 1st order relativistic correction. For the lfs channels, a spatial resolution δR of about $2 \div 3$ cm is obtained in comparison to δR_r of about 1 cm.

Almost the same features one can see in Fig.4, where the mapped to r_{eff} T_{rad} profile is shown and the measured one (and used for simulation). The radial (r_{eff}) bars also have almost the same value as for $T_{rad}(R_*)$, i.e. $\delta r_{eff} \simeq 2 \div 3$ cm. This spatial resolution of ECE diagnostic, with $\delta r_{eff}/r_{eff}$ up to 15% on low field side, is the natural lowest limit for W7-AS device.

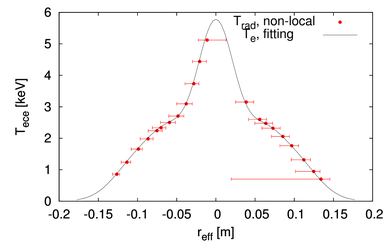

Figure 4a: *Radiative temperature profile mapped to the $T_{rad}(r_{eff})$ dependence.*

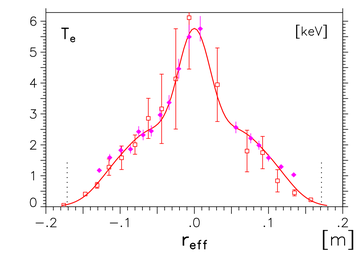

Figure 4b: *Experimentally measured T_e profile, obtained as a combination of Thomson scattering and ECE measurements results.*

The main results of the performed analyse:

- the degradation of the spatial resolution of the ECE data evaluation becomes significant at high electron temperatures;
- the T_{rad} profiles have a systematic shift to the high-field-side;
- a strong T_e gradient leads to an additional asymmetry in the ECE profiles.

For the W7-AS scenarios with a highly peaked T_e profile, only the high-field-side part of the ECE spectrum allows for an estimation of the "local" electron temperature.

References

[1] V. Tribaldos, *Spatial Resolution of ECE for JET Typical Parameters*, Report EFDA-JET (2000)

[2] G. Bekefi, *Radiation Processes in Plasmas* (John Willey & Sohns, New York, 1966)

[3] M. Bornatici at al., *Nuclear Fusion* **23** 1153 (1983)

[4] H. Maaßberg at al., *Phys. Plasmas* **7** 295 (2000)